SYNTHESIS OF TI-NI BASED HYDROGEN STORAGE ALLOY IN MOLTEN SALT

ANIK Mustafa

Eskisehir Osmangazi University, Metallurgical and Materials Engineering, Eskisehir, Turkey
manik@ogu.edu.tr

Abstract

A_2B type Ti-Ni hydrogen storage alloy, which has also dissolved Zr in it, was synthesized directly from TiO_2-ZrO_2-NiO mixture in the molten $CaCl_2$ electrolyte by the electro-deoxidation method at 900 °C. Sintering of the oxide mixture at 1100 °C for 2 h did not cause formation of any mixed type Ti-Zr-Ni oxide. Short time electro-deoxidation (< 5 h) yielded Ti_3O_5, $CaTiO_3$, $CaZrO_3$, Ni and Ti_2O_3 formations upon reduction of the sintered oxide mixture. Extension of the electro-deoxidation time up to 10 h caused disappearance of all these reduction products and there remained only TiO and Ti_2Ni phases. Presence of TiO lasted about 15 h and then the target alloy structure with 100 % Ti_2Ni phase was obtained with the maximum amount of dissolved Zr in it. The synthesized alloy was prepared as electrode and it was observed that it had maximum discharge capacity of 200 $mA\cdot h\cdot g^{-1}$. The capacity retention rate of the electrode, however, was relatively low probably due to the barrier action of the formed oxide layer on the alloy surface. As the charge/discharge cycle increases the thickness of the oxide layer also increases and then the in/out diffusion of the elemental hydrogen becomes difficult.

Keywords: Ti-Ni Alloys, electro-deoxidation, hydrogen storage, XRD

1. INTRODUCTION

Recently it was reported that many elements/compounds can be synthesized directly from their oxides/oxide mixtures in the molten salts [1-4]. This novel electrochemical process, which is known as Fray-Farthing-Chen (FFC) Cambridge process or electro-deoxidation, is accepted as revolutionary process since it provides great economical advantage especially if the multi-component alloy synthesis is achieved.

In this work $Ti_{0.85}Zr_{0.15}Ni$ ternary alloy was synthesized to obtain Ti_2Ni phase structure with the maximum amount of dissolved Zr in it by the molten salt electro-deoxidation method. The alloy development stages were characterized and the electrochemical hydrogen storage was applied to the final alloy structure.

2. MATERIALS AND METHODS

Required amounts of TiO_2, ZrO_2 and NiO powders were mixed homogeneously in anhydrous ethanol include 3% polyethylene glycol (PEG) with a planetary ball mill. The powder was then dried overnight at room temperature. Dried powder was cold pressed into pellets of 10 mm in diameter, under a pressure of 1.5 $ton\cdot cm^{-2}$. The oxide pellets were then sintered at 1100 °C for 2 h.

The electrochemical experiments were performed in a quartz cell which was located inside a homemade programmable electrical furnace. The upper end of the quartz cell was closed tightly with a quartz cover which has holes for the electrode leads, thermocouple, gas inlet and outlet. The quartz cell was continuously purged with Ar gas (100 - 150 $ml\cdot min^{-1}$) during the electro-deoxidation process.

100 g $CaCl_2$ was mixed with 1 g CaO and placed into graphite crucible. Before electro-deoxidation process $CaCl_2$-CaO powder mixture was dried under Ar gas. Drying was carried out by slow heating (about 1 $K\cdot min^{-1}$) to 150 °C and holding at 150 °C for 10 h and then slow heating to 300 °C and holding at 300 °C for 10 h and then finally slow heating to the target temperature of 900 °C for the electro-deoxidation experiments.

In order to fully remove the water and the possible redox-active impurities, pre-electrolysis were carried out at 1.5 V and 900 °C for 4 h. During the pre-electrolysis graphite crucible was used as anode and another graphite rod was used as cathode. For the electro-deoxidation experiments the graphite rod was removed from the cell and the prepared oxide pellet electrode was inserted into the quartz cell as a cathode. The electro-deoxidation was conducted at 3.0 V for 1 h, 5 h, 10 h, 15 h and 24 h at 900 °C.

After the electro-deoxidation experiments the pellet electrodes were removed from the molten melt and they were located in the upper part of the quartz cell which was cooled down by keeping the Ar gas purging. The solidified salt on the pellet was washed out by tap water. After slight surface grinding the pellets were kept in 1 M HCl for about 1 h. Finally the deoxidized pellet samples were dried at 100 °C for 24 h under vacuum.

Working electrodes were prepared by mixing 0.2 g alloy powder with 0.6 g nickel powder and then cold pressing into pellets of 10 mm in diameter, under a pressure of 10 $ton\cdot cm^{-2}$. Hg/HgO reference electrode was used to set up a three-electrode cell in 6 M KOH solution. Tests were performed with PARSTAT Model 2273 potentiostat/galvanostat unit. The charge current density was 100 $mA\cdot g^{-1}$ and the charging was carried out down to the severe gassing potential. The discharge current density was 25 $mA\cdot g^{-1}$ and the discharge cut-off potential was -0.6 $V_{Hg/HgO}$. The excitation voltage was 10 mV (peak to peak) and the applied frequency varied from 100 kHz to 0.01 Hz in the electrochemical impedance measurements.

The phase structure of the alloy powders was examined by the X-ray diffractometer (Bruker axs D8) using Cu Kα radiation. The powder morphologies were observed by ZEISS SUPRATM 50 VP Scanning Electron Microscope (SEM).

2.1. Structural and Morphological Characteristics

Scanning electron micrographs of the as-sintered oxide powder and the deoxidized powder (for 24 h) are provided in **Figure 1**. As-sintered powder has typical fine oxide powder appearance in **Figure 1a**. At the end of 24 h electro-deoxidation process, however, the typical large crystalline metallic powder morphology develops as in **Figure 1b**.

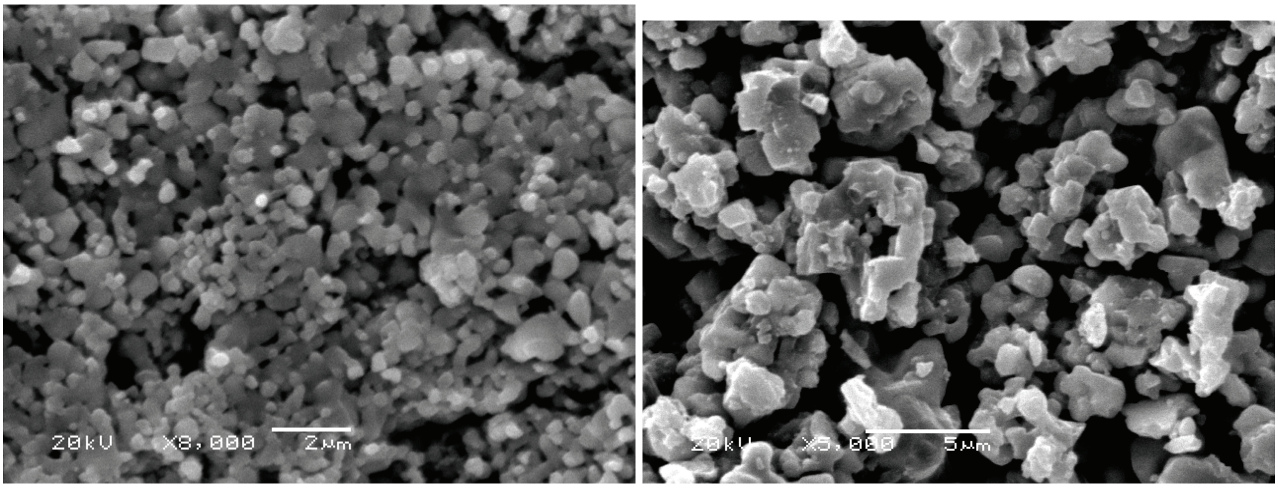

a) b)

Figure 1 Powder morphologies after (a) sintering and (b) electro-deoxidation for 24 h

The overlaid X-ray diffraction (XRD) patterns of the as-sintered, 1 h and 5 h deoxidized powders are shown in **Figure 2**. As-sintered powder has typical peaks of TiO_2, ZrO_2 and NiO. Upon deoxidation up to 5 h the intensities of these peaks reduce significantly and some of them disappear totally. Ti_3O_5, $CaTiO_3$, $CaZrO_3$, Ni and Ti_2O_3 form as the deoxidation products, within 5 h, according to the XRD peaks in **Figure 2**. The electro-deoxidation process in this period of time can be described by the following reactions:

$$4TiO_2 + Ca^{2+} + 2e^- = CaTiO_3 + Ti_3O_5 \quad (1)$$

$$2ZrO_2 + Ca^{2+} + 4e^- = CaZrO_3 + Zr + O^{2-} \quad (2)$$

$$NiO + 2e^- = Ni + O^{2-} \quad (3)$$

$$2Ti_3O_5 + 2e^- = 3Ti_2O_3 + O^{2-} \quad (4)$$

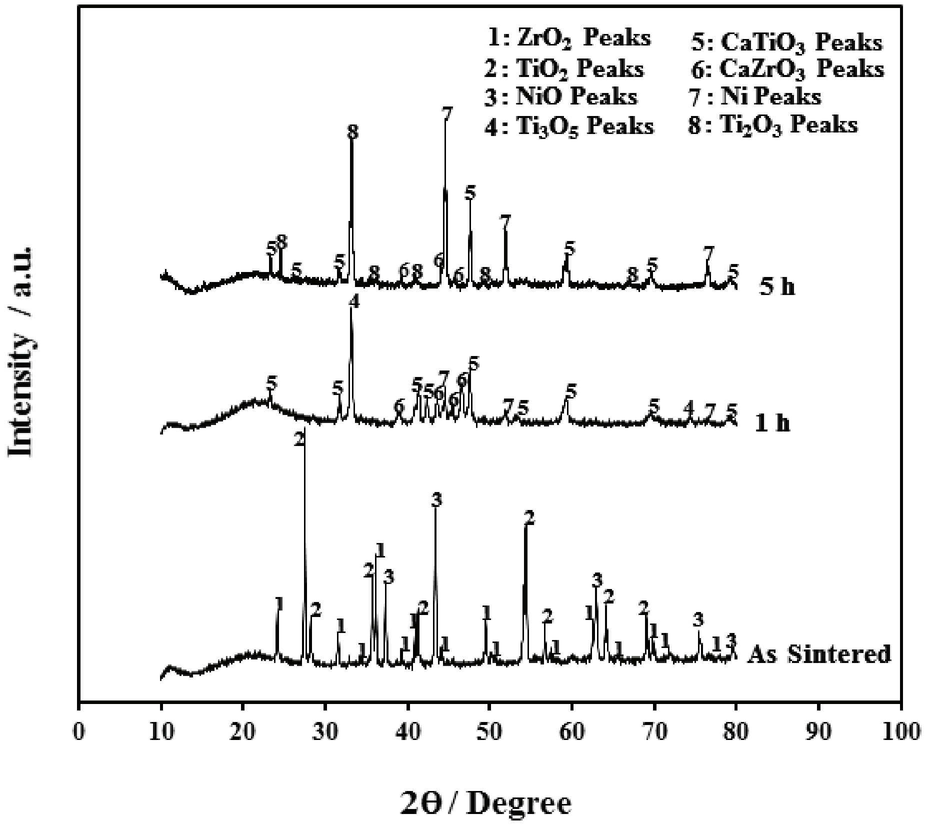

Figure 2 XRD patterns of the samples after sintering and electro-deoxidation for 1 h and 5 h

The XRD patterns of the powders after 10 h, 15 h and 24 h deoxidations are given in **Figure 3**. TiO as the only remaining oxide and the equilibrium Ti_2Ni phase appear after 10 h deoxidation process. Upon increase in the deoxidation time up to 15 h, the number of peaks belonging to the equilibrium Ti_2Ni phase increases and finally the target alloy structure, which has only equilibrium Ti_2Ni phase, is obtained after 24 h deoxiation in **Figure 3**. In this period of time the electro-deoxidation pathway can be estimated as in the following:

$$Ti_2O_3 + 2e^- = 2TiO + O^{2-} \quad (5)$$

$$CaTiO_3 + 2e^- = TiO + Ca^{2+} + 2O^{2-} \quad (6)$$

$$CaZrO_3 + 4e^- = Zr + Ca^{2+} + 3O^{2-} \quad (7)$$

$$2TiO + Ni + 4e^- = Ti_2Ni + 2O^{2-} \quad (8)$$

Despite the appearance of elemental Zr as the reaction product in Reactions (2) and (7), Zr peaks are not observable in **Figures 2** and **3**. The absence of Zr peaks may arise from both too low amount of Zr to be detected by the X-ray technique and the dissolution of Zr in the main phase. According to the Ti-Zr-Ni ternary phase diagram [5] Ti_2Ni phase (π′ phase [5]) has Zr solubility at around 8 atomic %. In fact the composition of the target alloy ($Ti_{0.85}Zr_{0.15}Ni$) was selected to obtain Ti_2Ni phase with the maximum amount of dissolved Zr in it. It is obvious from **Figure 3** that after 24 h electro-deoxidation process the desired alloy structure was obtained.

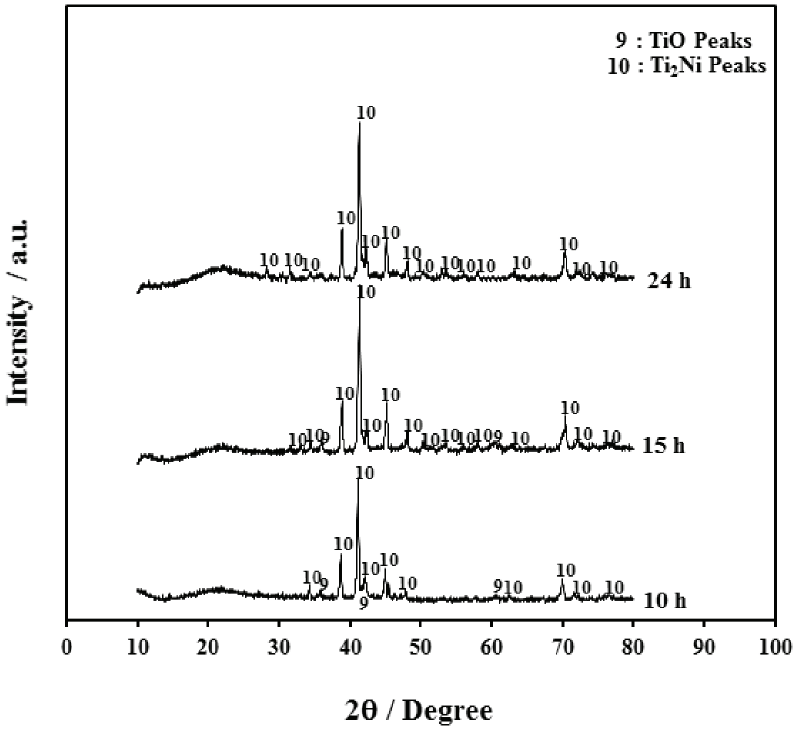

Figure 3 XRD patterns of the samples after electro-deoxidation for 10 h, 15 h and 24 h

2.2. Hydrogen Storage Characteristics of the Developed Alloy

The variations in the discharge capacities of 24 h electro-deoxidized sample (Ti_2Ni alloy) depending on the charge/discharge cycle numbers are indicated in **Figure 4**. Alloy needs few cycles for activation to reach its maximum discharge capacity. After reaching to 200 $mA \cdot h \cdot g^{-1}$, the discharge capacity decays down to 85 $mA \cdot h \cdot g^{-1}$ with 20 charge/discharge cycles. Obviously there is rapid degradation in Ti_2Ni electrode performance as also reported previously [6]. The sharp decay in the discharge capacity curve in **Figure 4** is probably due to barrier action of the thickening oxide/hydroxide layer makes hydrogen in and out diffusion difficult. The oxide/hydroxide layer on the Ti_2Ni-hydride electrode gets thicker after every charge/discharge cycle and thus the performance of the electrode degrades.

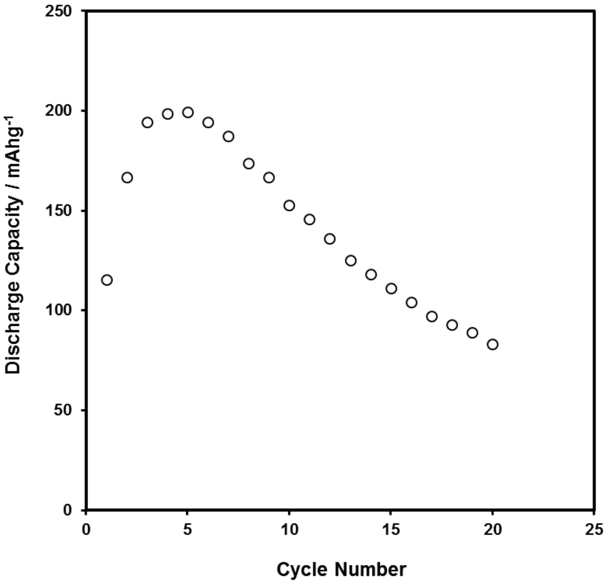

Figure 4 Discharge capacities of developed alloy depending on the charge/discharge cycles

3. CONCLUSIONS

- Stoichiometric oxides TiO_2, ZrO_2 and NiO reduced to Ti_3O_5, $CaTiO_3$, $CaZrO_3$, Ni and Ti_2O_3 within 5 h electro-deoxidation process.
- Extension of the electro-deoxidation time to 10 h caused formations of TiO and equilibrium Ti_2Ni phase.
- After 24 h electro-deoxidation the target alloy with equilibrium Ti_2Ni phase structure and the maximum amount of the dissolved Zr in it was obtained.
- The synthesized alloy had maximum discharge capacity of 200 $mA{\cdot}h{\cdot}g^{-1}$. Upon increase in the charge/discharge cycles, however, the discharge capacity decayed sharply.

REFERENCES

[1] CHEN, G. Z., FRAY, D. J., FARTHING T. W. Direct electrochemical reduction of titanium dioxide to titanium in molten chloride. *Nature*, 2000, vol. 407, pp. 361-364.

[2] FRAY, D. J., CHEN, G. Z. Reduction of titanium and other metal oxides using Electrodeoxidation. *Materials Science and Technology*, 2004, vol. 20, pp. 295-300.

[3] MOHANDAS K. S., FRAY, D. J. FFC Cambridge process and removal of oxygen from metal-oxygen systems by molten salt electrolysis: an overview. *Transactions of Indian Institute of Metals,* 2004, vol. 57, pp. 579-592.

[4] SCHWANDT C., FRAY, D. J. Determination of the kinetic pathway in the electrochemical reduction of titanium dioxide in molten calcium chloride. *Electrochimica Acta*, 2005, vol. 51, pp. 66-76.

[5] GUPTA K. P. The Ni-Ti-Zr System. *Journal of Phase Equilibria*, 1999, vol. 20, pp. 441-448.

[6] ZAVALIY I., WOJCİK G., MLYNAREK G., KOPCZYK M. Phase-structural characteristics of $(Ti_{1-x}Zr_x)_4Ni_2O_{0.3}$ alloys and their hydrogen gas and electrochemical absorption-desorption properties. *Journal of Alloys and Compounds*, 2001, vol. 51, pp. 124-131.